



Comprehensive impact of pre-treatment methods on white radish quality, water migration, and microstructure

Bixiang Wang, Yuanlong Jia, Yue Li, Xuan Jiao, Yang He^{*}, Liankui Wen^{*}, Zhitong Wang^{*}

Department of Food Science and Engineering, Jilin Agricultural University, Changchun 130118, China.

ARTICLE INFO

Keywords:

White radish
Pre-treatment
Water migration
Microstructure
Vegetables
Quality

ABSTRACT

The preprocessing stage is crucial in vegetable processing, significantly influencing the final product's quality. This study investigates the effects of various pre-treatment methods, including cutting, blanching, osmotic, and ultrasound-assisted osmotic treatment, on the quality characteristics, water migration, and microstructure of white radish. The results showed that osmosis and ultrasound-assisted osmosis has the least effect on the total color difference (ΔE) and the greatest water loss (WL) ($p < 0.05$); blanching has the least effect on the hardness and eutectic points ($p < 0.05$); and the blanching-ultrasound-assisted osmosis has the greatest solid gain ($p < 0.05$). The increase of WL led to a decrease in hardness (-0.82). By analyzing the quality characteristics of different pre-treatment methods, contributing to the development of suitable pre-treatment methods for different products and optimization pre-treatments according to requirements. The mechanism of quality characteristics of pre-treatments on products is the future research direction.

1. Introduction

White radish (*Raphanus sativus* L.), a cultivated variety within the Brassicaceae family (Luo et al., 2022), is a widely consumed vegetable due to its high yields and rich nutritional profile, including organic acids, vitamins, protein, and dietary fiber (FAO, 2022; Li et al., 2021). However, its high moisture content (about 95 %) makes it easy to rot during storage, so in addition to storage such as refrigeration or gas packaging, it is usually made into storage-resistant products by various processing techniques such as drying, sugar pickling and pickling (Kumakura et al., 2017). Pretreatment is a critical initial step in the drying process that significantly affects the final product's quality. Pretreatment is pivotal in determining the product's color, texture, and so on (Wang et al., 2021). The quality characteristics of the product after pretreatment will also affect the quality of the product after drying.

In order to facilitate the exchange of substances in the tissue and improve the quality of products. Vegetables are usually pre-treated with different methods (including cutting, blanching, osmosis, ultrasound-assisted osmosis) to promote the removal of some water. As the first step in vegetable processing, pretreatment can alter the microstructure of the samples, such as pore size and cell size (An, Sun, Li, et al., 2022; Tao, Han, Gao, et al., 2019; Wang et al., 2021), facilitating water loss, reducing energy consumption, and enhancing overall sensory quality,

including color, texture, and more (Jiang, Zhang, Devahastin, & Yu, 2021; Rojas, Silveira, & Augusto, 2019). Blanching and ultrasonic pre-treatment can enlarge the pores of the samples because ultrasound creates microchannels or adjacent cell fusion due to the loss of tissue integrity (Nowacka et al., 2019). Additionally, the cavitation effect generated by ultrasonic treatment accelerates the formation of micropores in the material, leading to increased pore size and promoting water loss. Blanching disrupts the integrity of cell membranes, enhancing water transfer within the tissue and reducing the sample's water-holding capacity, indicating that cell structure is related to mass transfer (Wang et al., 2023; Wang, Fang, Mujumdar, et al., 2017). It has been observed that osmotic treatment results in a reduction in moisture content and enhances the mass transfer of sugar and water between the osmotic solution and vegetables. Similarly, studies by Xu et al. (2021) on ultrasonic pre-treatment of strawberry slices revealed that the transverse relaxation time of the free water after ultrasonic pretreatment was significantly shortened, and the area of the free water (A3) was constantly decreasing (Xu, Jin, Zhang, & Chen, 2017). US pre-treatment has been studied many years (Andreou, Dimopoulos, Dermesonlouoglou, & Taoukis, 2020), yet there remains a need for a more in-depth investigation into the effects of ultrasound on water migration within vegetables. The aforementioned researchers have conducted various pre-treatments on vegetables, each influencing the quality

^{*} Corresponding authors.

E-mail addresses: heyang200704@jlau.edu.cn (Y. He), wenliankui@163.com (L. Wen), wangzhitong03@163.com (Z. Wang).

characteristics of the produce. These studies contribute to identifying suitable pre-treatment methods for vegetables in the context of further processing. The various pretreatments, including cutting, blanching, osmosis, and ultrasound-assisted osmosis, alter the microscopic structure of vegetables to facilitate water loss, reduce energy consumption, and enhance sensory quality. However, there are relatively few reports on the combined use of these comprehensive pretreatment methods, and further research is still needed.

This paper evaluates the quality, water migration, and internal microstructure of samples subjected to various treatments: cutting, blanching, osmosis, ultrasound-assisted osmosis, and blanching-followed-by-ultrasound-assisted osmosis. It further analyzes the correlation among these overall factors to deeply explore the impacts of different pre-treatments on the microstructure, water migration, and product quality of white radish. This provides a crucial opportunity to elucidate the pre-treatment mechanism of white radish from a more realistic perspective.

2. Materials and methods

2.1. Raw materials

White radishes (*Raphanus sativus* L.) (baiyudagen variety) were purchased from a local market in Changchun, China. Fresh, bright color, uniform size, without any disease, pests or mechanical damage of white radishes were selected as the experimental raw material. The initial moisture content was 95.85 ± 0.08 % (wet basis, w.b.).

2.2. Chemical reagents

Fixative for TEM was acquired from Servicebio Biotechnology Co., Ltd. (Wuhan, China). EMBed 812 was bought from Structure Probe, Inc. (California, USA). OsO₄ was obtained from Ted Pella, Inc. (California, USA). Glucose, potassium bromide, ethanol, and acetone were purchased from Sinaopharm Group Chemical Reagent Co., Ltd. (Shanghai, China).

2.3. Samples pre-treatments

2.3.1. Cutting

The samples were cut in transversal cutting (TC) and longitudinal

cutting (LC) into pieces of 2.5 cm in diameter and 0.5 cm in thickness and strips of 5 cm × 0.8 cm × 0.5 cm, both weighing 6.0 ± 0.2 g.

2.3.2. Blanching

The cut samples were placed in blanching water (70 °C) for 15 min.

2.3.3. Osmosis

The samples were placed in 20 % glucose osmotic solution with a osmotic material to liquid ratio of 1:10 and permeated for 30 min.

2.3.4. Ultrasound-assisted osmosis

The cutting samples were placed in 20 % osmotic glucose solution (w/v 1:10) and ultrasound for 30 min at 180 W (20 kHz). The temperature changes before and after ultrasound was <2 °C.

2.3.5. Combined treatment

Blanching-ultrasound-assisted osmosis. The cutting samples were placed in blanching water (70 °C) for 15 min. The blanching samples were placed in 20 % osmotic glucose solution (w/v 1:10) and ultrasound for 30 min at 180 W. The temperature changes before and after ultrasound was <2 °C.

The specific operation conditions are shown in the following [Table 1](#).

2.4. Quality characteristics

2.4.1. Color measurement

Color difference of pre-treated samples was measured by colorimeter (HunterLab, Reston, VA, USA). The calculation formulas are as follows:

$$\Delta E = \left((L^* - L_0^*)^2 + (a^* - a_0^*)^2 + (b^* - b_0^*)^2 \right)^{1/2}$$

$$(\text{Whiteness}) = 100 - \sqrt{(100 - L^*)^2 + a^{*2} + b^{*2}}$$

$$C = \sqrt{a^{*2} + b^{*2}}$$

The L*, a*, b* value present for brightness/blackness, redness/greenness, and yellowness/ blueness, respectively. ΔE value represents the color difference value, whiteness represents the white degree of white radish, chroma (C) represents the chromaticity ([Chao, Li, & Fan, 2022](#)).

Table 1
Different pre-treatment conditions.

| Pre-treatments | Cutting | | | | Blanching | Osmotic | Ultrasound |
|----------------|-------------------|-------------------|--------------------|--------------------|-----------|---------|------------|
| | Transversal piece | Transversal strip | Longitudinal piece | Longitudinal strip | | | |
| CTP | * | – | – | – | – | – | – |
| CTS | – | * | – | – | – | – | – |
| CLP | – | – | * | – | – | – | – |
| CLS | – | – | – | * | – | – | – |
| CBTP | * | – | – | – | * | – | – |
| CBTS | – | * | – | – | * | – | – |
| CBLP | – | – | * | – | * | – | – |
| CBLS | – | – | – | * | * | – | – |
| COTP | * | – | – | – | – | * | – |
| COTS | – | * | – | – | – | * | – |
| COLP | – | – | * | – | – | * | – |
| COLS | – | – | – | * | – | * | – |
| COUTP | * | – | – | – | – | * | * |
| COU TS | – | * | – | * | – | * | * |
| COULP | – | – | * | – | – | * | * |
| COULS | – | – | – | * | – | * | * |
| CBOUTP | * | – | – | – | * | * | * |
| CBOU TS | – | * | – | – | * | * | * |
| CBOULP | – | – | * | – | * | * | * |
| CBOULS | – | – | – | * | * | * | * |

Note: “–” represents no pretreatment under this condition. “*” represents pretreatment under this condition. C: Cutting; T: Transversal; L: Longitudinal; P: Piece; S: Strip; B: Blanching; O: Osmotic; U: Ultrasound. The combination of capital letters represents joint processing.

2.4.2. Textural structure

The hardness, brittleness, chewiness, and elasticity of the pre-treatment samples were measured by a texture analyzer (TA.new plus, Shanghai RuiFen International Trade Co., Ltd., Shanghai, China) with a 50 kgf load cell (490.3 N) and a cylindrical probe (P/36). The pre-test, test and post-test speeds were 2.0, 1.0, and 1.0 mm/s, respectively.

2.4.3. Water loss (WL) and solid gain (SG)

The equation for the WL and solid gain SG of white radish samples is expressed as follows (Ozen, Dock, Ozdemir, & Floros, 2002).

$$WL = \frac{(W_0 - W_t) + (S_t - S_0)}{W_0} \times 100$$

$$SG = \frac{S_t - S_0}{W_0} \times 100$$

WL is the water loss, W_0 is the initial fresh weight of white radish (g), W_t is the fresh weight at a certain time (g), S_t is the dry weight at a certain time (g), and S_0 is the initial dry weight (g).

2.5. Moisture migration

2.5.1. Low-field nuclear magnetic resonance (LF-NMR) spectroscopy

All pre-treatment samples were placed in a 40 mm diameter measuring tube, and the migration changes of water after pre-treatment were analyzed using a Newmax nuclear magnetic resonance (NMR) analyzer (MiniMR-60, New Mai Electronic Technology Co., Ltd., Beijing, China), and the relaxation time (T_2) was measured using the CPMG sequence determination.

2.5.2. Differential scanning calorimetry (DSC)

The thermal properties of the samples were determined by DSC (Q200, TA, Delaware, USA). Before the measurement, the instrument was calibrated using an indium standard. Subsequently, a 3 mg aliquot of the pre-treated sample was deposited into a solid aluminum crucible. The glass transition temperature (T_g) of the sample was then determined utilizing an empty crucible as the control reference. The thermal characteristics were measured by first decreasing the temperature at a rate of 10 °C/min to -80 °C, where it was then allowed to equilibrate for 5 min. The temperature was then increased to 50 °C at a rate of 10 °C/min. The scanned results were analyzed using the software (Universal Analysis, TA, Delaware, USA).

2.6. Microstructure

2.6.1. Optical microscope

The microstructure changes of the sample after different pre-treatments were observed using optical microscope. The samples were cut to a thickness of 1 mm and a length of 3 mm, and then placed under an optical microscope (DM1000, LEICA, AG, Germany) for observation. The image magnification was 100 × .

2.6.2. Scanning electron microscopy (SEM)

SEM was used to observe the microstructural changes on the surface of the samples. Following the drying process, the samples were meticulously sectioned into smaller fragments. Subsequently, these fragments were affixed to the sample scanning stage via a layer of double-sided conductive adhesive tape. Afterward, they were sprayed with a layer of gold and placed in the SEM (SSX-550, SHIMADZU, Kyoto, Japan) sample chamber for observation, with a voltage setting of 10 KV and the magnification of 100 × (Zhou et al., 2020).

2.6.3. Transmission electron microscopy (TEM)

The samples were cut into 70 nm slices with an ultrathin slicer (Leica UC7, Leica, Weztlar, Germany). The samples were washed by ultrapure water for three times, and the filter paper was slightly sucked dry. The

copper mesh slices were put into a copper mesh box and dried overnight at room temperature. The samples were observed under a TEM (HITACHI HT7800/HT7700, Tokyo, Japan), and images were collected for analysis. The magnification was 6000 × .

2.6.4. Fourier transform infrared (FT-IR) spectroscopic

An accurately measured quantity of 2 mg of dried cell wall material was combined with 200 mg of dried potassium bromide (KBr). The mixture was subsequently finely ground using an agate mortar to ensure homogeneity. The resulting mixture was then pressed into tablets with a pressure of 15–20 MPa for 1 min. Subsequently, the samples were scanned using FT-IR (model IR Prestige-21, Shimadzu, Tokyo, Japan) in the range of 500–4000 cm^{-1} .

2.7. Statistical analysis

The texture analysis of white radish samples was repeated eight times, and all other measurements were performed three times. All data were presented as the mean values ± standard deviations (SD). Data variance was analyzed by using SPSS software (SPSS24, Chicago, USA), and Duncan's multi-range test was performed (significant at $p < 0.05$). In addition, images were drawn using Origin2021 (OriginLab Co., Northampton, Massachusetts, USA).

3. Results and discussion

3.1. Pre-treatments effect on quality

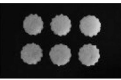

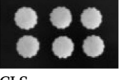
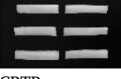
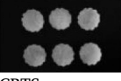
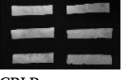

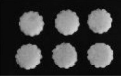


3.1.1. Color analysis

Compared to cutting (CTP, CTS, CLP, CLS) samples, all pre-treatment samples had lower L^* value ($p < 0.05$), where blanching and ultrasound-assisted osmosis samples (CBOU) had the lowest L^* and C values ($p < 0.05$), the largest ΔE value ($p < 0.05$), osmosis samples (COU) had the largest whiteness value (Table 2). The blanching (CB) and ultrasound-assisted osmosis samples (COU) has a greater effect on the color difference values. This is due to the reaction of enzymatic browning, caramelization and browning after ultrasonic-assisted infiltration and blanching (Nokuthula, Sephora, Faith, & Dharini, 2024; Wang et al., 2021). This study confirmed this point. The reason of color protection is that sugar can effectively inhibit the role of polyphenol oxidase in vegetable after cutting (Ahmed, Qazi, & Jamal, 2016). Colorless clear glucose osmotic solution was used in this study, which may account for the small color change. The research indicates that different pretreatment methods have varying effects on the color of fruits and vegetables. In the study by Wang et al. (2022) on apples, they found that apple slices treated with hot water blanching exhibited minimal color changes during storage, whereas untreated apple slices showed significant browning. In this study, it was discovered that the combination of blanching and ultrasound treatment had the greatest impact on color, indicating that this combined treatment had a more pronounced effect on color than either blanching or ultrasound treatment alone.

3.1.2. Texture profile analysis


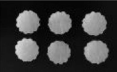

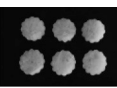
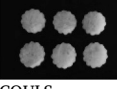

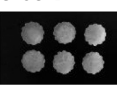
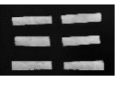
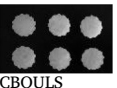
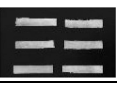
Compared to cutting samples, hardness decreased in all treatment groups, with the smallest change in hardness in CB samples and the largest change in hardness in COU samples ($p < 0.05$) (Table 1). We believe that the decrease in hardness of the sample after blanching is due to the softening of the cell wall pectin and the depolymerisation of β after blanching (Wang et al., 2021). The hardness of blanching-ultrasound-assisted osmosis samples (CBOU) was higher than that osmosis samples, because blanching and ultrasound increase the glucose osmosis, so the solids content of the sample increases. Furthermore, the resilience, springiness, hardness, chewiness, gumminess, and cohesiveness were greater for TC samples than for LC samples. Fibers in xylem mainly play a supporting role. This may be because different cutting methods make the fiber direction different, and the transverse cutting

Table 2
Quality parameters of white radish after pre-treatment.

| Pre-treatments | L* | a* | b* | ΔE | White | Chroma (C) | Resilience | Springiness | Hardness | Chewiness | Gumminess | Cohesiveness | WL (%) | SG (%) | Tg' | ΔHm |
|---|-----------------|------------------|------------------|----------------|----------------|-----------------|-----------------|-----------------|---------------------|-----------------------|---------------------|------------------|-----------------|----------------|-----------------|-------------------|
| CTP  | 65.11 ± 0.09 c | -0.95 ± 0.01 ab | 2.73 ± 0.05 de | - | 64.99 ± 0.09 c | 2.89 ± 0.04 efg | 0.84 ± 0.01 a | 0.90 ± 0.03 ab | 4113.17 ± 90.69 a | 3504.26 ± 197.19 a | 3901.22 ± 100.40 a | 0.95 ± 0.01 a | - | - | -5.33 ± 0.50 cd | -195.80 ± 2.91 g |
| CTS  | 65.06 ± 0.03 c | -0.10 ± 0.05 abc | 2.84 ± 0.28 d | - | 64.93 ± 0.05 c | 3.02 ± 0.24 def | 0.80 ± 0.01 ab | 0.89 ± 0.01 abc | 3653.61 ± 29.31 b | 3007.11 ± 61.06 b | 3392.36 ± 27.81 b | 0.93 ± 0.01 a | - | - | -5.44 ± 0.36 cd | -231.37 ± 1.01 h |
| CLP  | 67.34 ± 0.06 b | -1.07 ± 0.02 bcd | 4.85 ± 0.03 b | - | 66.96 ± 0.05 b | 4.97 ± 0.03 b | 0.81 ± 0.01 ab | 0.91 ± 0.01 ab | 3855.36 ± 36.84 b | 3373.44 ± 72.65 a | 3703.90 ± 55.73 a | 0.96 ± 0.01 a | - | - | -5.07 ± 0.27 c | -200.92 ± 0.96 g |
| CLS  | 67.77 ± 0.10 b | -1.16 ± 0.03 def | 4.62 ± 0.05 bc | - | 67.42 ± 0.10 b | 4.76 ± 0.04 bc | 0.75 ± 0.02 b | 0.93 ± 0.02 a | 3187.67 ± 48.82 c | 2744.64 ± 90.23 b | 2947.45 ± 42.67 b | 0.93 ± 0.02 a | - | - | -3.60 ± 0.31 ab | -189.72 ± 1.29 fg |
| CBTP  | 55.91 ± 0.35 g | -1.52 ± 0.03 ij | 0.34 ± 0.11 g | 9.52 ± 0.36 b | 55.88 ± 0.35 g | 1.57 ± 0.02 h | 0.64 ± 0.02 c | 0.79 ± 0.02 de | 2646.41 ± 38.89 d | 1645.34 ± 51.96 c | 2082.94 ± 26.14 c | 0.79 ± 0.01 cde | 4.80 ± 0.36 e | -1.44 ± 0.17 f | -3.14 ± 0.34 a | -160.03 ± 4.82 de |
| CBTS  | 56.26 ± 0.18 g | -1.6 ± 0.02 j | 0.45 ± 0.05 g | 9.16 ± 0.18 b | 56.23 ± 0.17 g | 1.66 ± 0.02 h | 0.61 ± 0.02 cde | 0.79 ± 0.02 de | 2583.24 ± 137.47 d | 1514.87 ± 106.18 cde | 1921.58 ± 119.72 cd | 0.74 ± 0.01 cdef | 5.65 ± 0.81 e | -1.70 ± 0.10 f | -2.90 ± 0.32 a | -166.28 ± 8.98 e |
| CBLP  | 59.55 ± 0.77 f | -1.87 ± 0.02 k | 2.66 ± 0.13 de | 5.64 ± 0.76 c | 59.42 ± 0.76 f | 3.26 ± 0.09 de | 0.62 ± 0.02 cd | 0.81 ± 0.03 cd | 2127.43 ± 121.52 ef | 1359.96 ± 152.26 cdef | 1676.60 ± 135.03 de | 0.79 ± 0.02 cde | 4.02 ± 0.43 e | -1.54 ± 0.14 f | -2.45 ± 0.49 a | -165.1 ± 3.63 e |
| CBLS  | 55.96 ± 0.18 g | -1.82 ± 0.06 k | 1.67 ± 0.04 ef | 9.23 ± 0.18 b | 55.89 ± 0.18 g | 2.47 ± 0.07 efg | 0.55 ± 0.04 ef | 0.79 ± 0.01 de | 2120.47 ± 99.46 ef | 1203.32 ± 96.03 efg | 1532.21 ± 136.30 e | 0.72 ± 0.03 ef | 9.02 ± 0.63 d | -1.71 ± 0.07 f | -2.59 ± 0.38 a | -167.81 ± 5.97 e |
| COTP  | 61.23 ± 0.27 e | -1.06 ± 0.03 a | 1.78 ± 0.04 def | 3.99 ± 0.27 d | 61.18 ± 0.26 e | 2.07 ± 0.04 fgh | 0.48 ± 0.01gh | 0.75 ± 0.03 def | 1090.57 ± 71.93 h | 634.55 ± 70.46 ij | 846.65 ± 66.81 g | 0.78 ± 0.01 cde | 13.80 ± 0.38 bc | 1.34 ± 0.02 de | -7.41 ± 0.14 ef | -139.8 ± 1.75 c |
| COTS  | 60.30 ± 0.03 ef | -0.93 ± 0.03 bcd | 2.467 ± 0.07 def | 4.81 ± 0.03 cd | 60.22 ± 0.03 f | 2.63 ± 0.06 efg | 0.32 ± 0.02 j | 0.69 ± 0.03 efg | 582.55 ± 13.00 i | 277.65 ± 8.90 k | 401.49 ± 3.42 h | 0.69 ± 0.01 f | 15.84 ± 0.02 ab | 1.97 ± 0.07 c | -5.2 ± 0.22 cd | -195.34 ± 3.80 g |

(continued on next page)

Table 2 (continued)

| Pre-treatments | L* | a* | b* | ΔE | White | Chroma (C) | Resilience | Springiness | Hardness | Chewiness | Gumminess | Cohesiveness | WL (%) | SG (%) | Tg' | ΔHm |
|---|----------------|------------------|-----------------|----------------|----------------|-----------------|-----------------|-----------------|---------------------|-----------------------|---------------------|------------------|------------------|----------------|-----------------|-------------------|
| COLP  | 67.36 ± 0.55 b | -1.33 ± 0.07 gh | 7.25 ± 1.06 a | 5.11 ± 1.10 cd | 66.50 ± 0.46 b | 7.38 ± 1.058 a | 0.61 ± 0.03 cde | 0.81 ± 0.02 cd | 2241.47 ± 136.21 ef | 1570.31 ± 111.80 cd | 1927.06 ± 99.80 cd | 0.86 ± 0.01 b | 16.86 ± 0.0041 a | 0.75 ± 0.04 e | -4.51 ± 0.48 bc | -189.32 ± 2.60 fg |
| COLS  | 68.98 ± 0.04 a | -1.25 ± 0.02 fg | 5.26 ± 0.02 b | 4.63 ± 0.03 cd | 68.51 ± 0.05 a | 5.41 ± 0.02 b | 0.47 ± 0.01 gh | 0.78 ± 0.03de | 1459.64 ± 59.33 g | 894.48 ± 58.07 ghi | 1140.79 ± 53.56 f | 0.78 ± 0.01 cde | 18.3481 ± 1.16 a | 1.58 ± 0.30 cd | -4.74 ± 0.31 c | -126.22 ± 1.31 b |
| COU TP  | 63.71 ± 0.17 d | -1.27 ± 0.01 fg | 3.76 ± 0.06 c | 1.77 ± 0.11 e | 63.50 ± 0.17 d | 3.96 ± 0.06 cd | 0.43 ± 0.01 h | 0.55 ± 0.02 h | 2090.11 ± 53.88 ef | 781.05 ± 41.93 hij | 1414.60 ± 34.29 ef | 0.68 ± 0.01 f | 16.78 ± 0.83 a | 1.24 ± 0.02 de | -9.29 ± 0.20 g | -129.37 ± 0.65 b |
| COU TS  | 59.90 ± 0.11 f | -1.23 ± 0.03 efg | 2.77 ± 0.07 de | 5.21 ± 0.11 cd | 59.79 ± 0.11 f | 3.03 ± 0.07 def | 0.27 ± 0.03 i | 0.57 ± 0.02 h | 1237.76 ± 27.36 gh | 280.36 ± 15.03 k | 489.82 ± 36.27 h | 0.40 ± 0.03 g | 17.99 ± 0.44 a | 0.94 ± 0.11 de | 5.76 ± 0.25 cd | -180.20 ± 2.37 f |
| COULP  | 65.65 ± 0.33 c | -1.08 ± 0.03 cd | 3.86 ± 0.13 c | 1.32 ± 0.20 e | 65.42 ± 0.31 c | 4.00 ± 0.13 cd | 0.57 ± 0.02 def | 0.68 ± 0.02 fg | 2396.01 ± 88.06 de | 1292.31 ± 122.33 def | 1904.14 ± 147.34 cd | 0.79 ± 0.03 cd | 16.35 ± 1.22 a | 0.93 ± 0.06 de | -5.28 ± 0.18 cd | -181.17 ± 1.56 f |
| COULS  | 59.54 ± 0.06 f | -1.12 ± 0.01 cde | 2.38 ± 0.03 def | 5.58 ± 0.06 c | 59.45 ± 0.06 f | 2.63 ± 0.03 efg | 0.32 ± 0.02 i | 0.62 ± 0.02 gh | 1151.57 ± 73.61 h | 489.82 ± 52.38 jk | 786.33 ± 63.31 g | 0.68 ± 0.01 f | 17.47 ± 0.92 a | 1.10 ± 0.05 de | -6.50 ± 0.22 de | -126.60 ± 2.44 b |
| CBOUTP  | 55.59 ± 0.15 g | -1.76 ± 0.04 k | 0.32 ± 0.03 g | 9.85 ± 0.15 b | 55.55 ± 0.15 g | 1.79 ± 0.03 gh | 0.52 ± 0.02 fg | 0.75 ± 0.02 def | 2170.22 ± 127.83 ef | 1218.42 ± 92.16 efg | 1613.38 ± 100.36 de | 0.74 ± 0.01 cdef | 11.74 ± 0.92 c | 4.82 ± 0.22 b | -10.63 ± 0.20 h | -118.37 ± 1.84 b |
| CBOUTS  | 53.11 ± 0.20 h | -1.42 ± 0.01 fi | 0.42 ± 0.03 g | 12.23 ± 0.19 a | 53.08 ± 0.20 h | 1.48 ± 0.02 h | 0.53 ± 0.01 fg | 0.76 ± 0.02 def | 1954.39 ± 86.37 f | 1078.62 ± 57.52 fgh | 1419.56 ± 50.79 ef | 0.73 ± 0.01 def | 12.93 ± 0.18 c | 6.13 ± 0.09 a | -8.20 ± 0.25 f | -151.01 ± 3.11 d |
| CBOLP  | 51.82 ± 0.25 i | -1.55 ± 0.05 j | 1.46 ± 0.11 f | 13.36 ± 0.26 a | 51.77 ± 0.25 i | 2.14 ± 0.07 efg | 0.57 ± 0.01 def | 0.83 ± 0.04 bcd | 2111.14 ± 47.85 ef | 1404.94 ± 101.28 cdef | 1690.73 ± 43.93 de | 0.80 ± 0.01c | 13.53 ± 0.28 bc | 5.06 ± 0.56 b | -8.15 ± 0.19 f | -152.07 ± 2.91 d |
| CBOLLS  | 56.15 ± 0.14 g | -1.49 ± 0.06 ij | 1.57 ± 0.03 f | 9.04 ± 0.14 b | 56.10 ± 0.14 g | 2.17 ± 0.05 efg | 0.53 ± 0.01 fg | 0.79 ± 0.02 de | 1900.86 ± 71.58 f | 1112.68 ± 81.34 fgh | 1403.01 ± 66.42 ef | 0.74 ± 0.01 cdef | 12.49 ± 0.46 c | 5.39 ± 0.17 b | -7.45 ± 0.49 ef | -92.14 ± 2.27 a |

Note: C: Cutting; T: Transversal; L: Longitudinal; P: Piece; S: Strip; B: Blanching; O: Osmotic; U: Ultrasound. The combination of capital letters represents joint processing.

sample fiber has stronger binding force on the moisture and composition of the sample.

3.1.3. WL and SG analysis

The maximum value of WL is ultrasound-assisted osmosis samples, the minimum value is blanching samples. The study by Jiang et al. (2021) on strawberries found that ultrasonic osmosis significantly increased WL, which is consistent with the present study where ultrasonic osmosis resulted in the greatest WL. This is similar to the research conducted by Shafiq et al. (2022), where samples that underwent

osmotic pre-treatment followed by drying exhibited lower moisture content. Researchers attributed this to the rapid drying after fruit immersion, the formation of microcracks, and the removal of waxes and lipids from the fruit skin, all of which facilitated rapid moisture evaporation. The maximum value of SG is blanching and ultrasound-assisted osmosis samples, and the minimum value is blanching samples (Fig. 1). This indicates that ultrasonic osmosis pretreatment not only promotes water extraction from fruits but also from vegetables. We often think of WL values as the opposite of SG values, but our study found that this is not the case. WL significantly increased after ultrasound-assisted

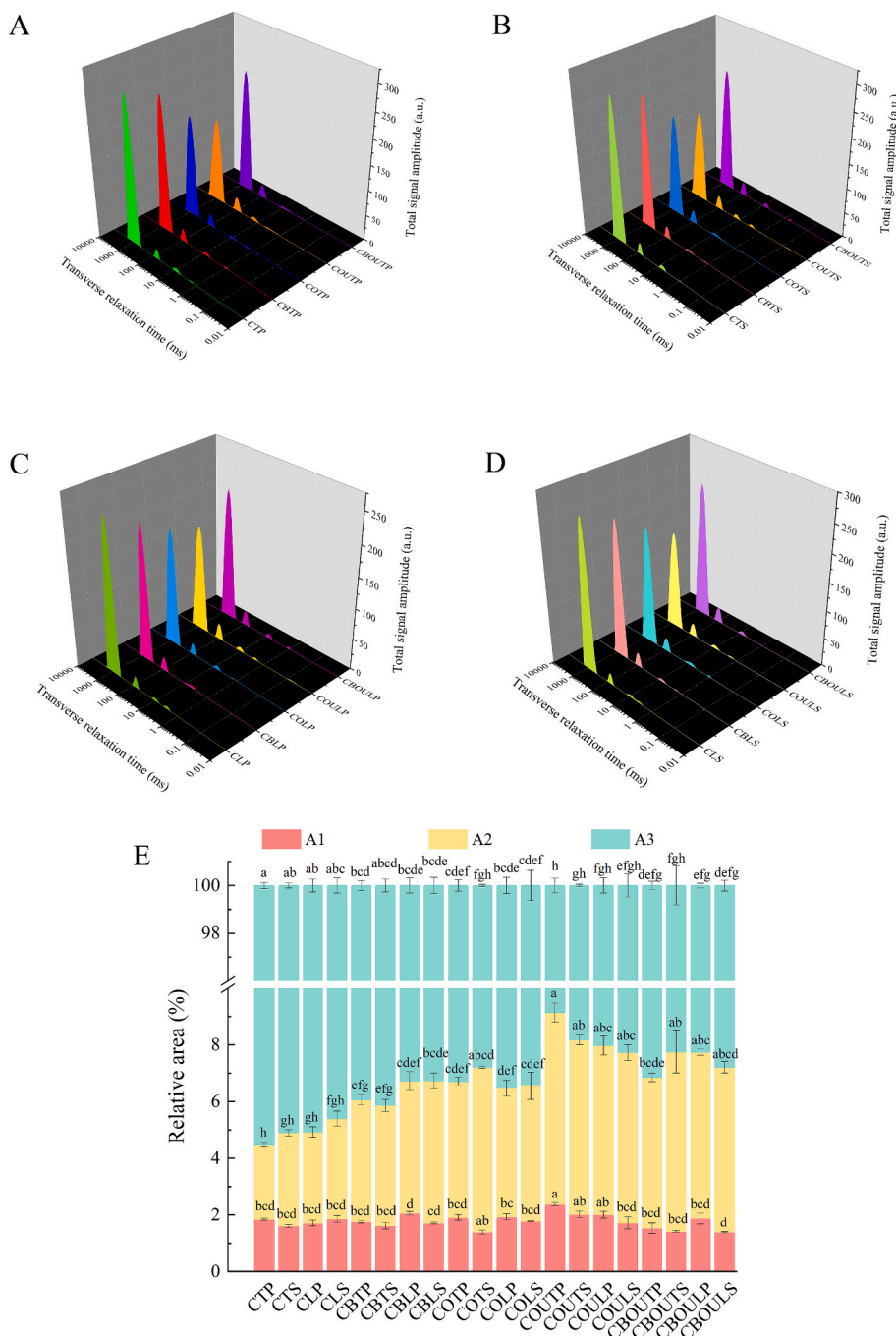


Fig. 1. Changes in water migration after pre-treatment of white radish. (C: Cutting; T: Transversal; L: Longitudinal; P: Piece; S: Strip; B: Blanching; O: Osmotic; U: Ultrasound. The combination of capital letters represents joint processing. A: Water migration changes in CTP, CBTP, COTP, COUTP, CBOUTP group; B: Changes in water transport in CTS, CBTS, COTS, COUTS, CBOUTS group; C: Changes in water migration in CLP, CBTP, COTP, COUTP, CBOUTP group; D: Changes in water transport in CLS, CBLS, COTS, COUTS, CBOUTS group; E: Stacked plot of water relaxation area).

osmotic pre-treatment. The WL directly reduces the swelling pressure (An, Lv, Li, Wang, & Wang, 2023), which is consistent with the decrease in sample hardness after pretreatment. In our study, the samples subjected to CBOU samples exhibited the most significant increase in specific gravity (SG) ($p < 0.05$). This finding aligns well with the observations made by Nowacka et al. (2019), who reported that during osmotic dehydration, the softening of pulp resulting from cutting and blanching facilitated bidirectional mass transfer, leading to an elevation in soluble solid content post-osmotic dehydration. Similarly, Ding's research (Ding et al., 2024) echoed this notion, indicating that ultrasonic pretreatment enhances water loss and accelerates the drying process, which is consistent with our results. Furthermore, our study delves deeper into the mechanism behind these observations. The microporous channel effect of ultrasound, as described by Bozkir, Rayman Ergün, Serdar, Metin, and Baysal (2019), creates tiny channels within the cellular tissue, facilitating the transfer of substances and altering tissue porosity. This, in turn, leads to increased water loss and a subsequent rise in SG. Additionally, the sponge effect of ultrasound, as reported by Zhang et al. (2020), aids in the removal of air from the vegetables, contributing to the maceration process. By comparing and contrasting these findings with our own, we can infer that the combined effects of blanching and ultrasound-assisted osmosis not only enhance water loss and drying efficiency but also alter the structural properties of the fruit or vegetable tissue, leading to more efficient mass transfer and improved product quality.

3.2. Effects of pre-treatments on changes in water migration

3.2.1. Low-field nuclear magnetic resonance (LF-NMR) analysis

The T2 relaxation times delineate the different states of water within a sample: T21 (0.01–10 ms) corresponds to bound water, T22 (10–100 ms) represents immobilized water, and T23 (100–10,000 ms) is indicative of free water, as elucidated by Fan and Zhang (2019) and Chen et al. (2020). Notably, during the entire pre-treatment process, the T21 exhibits the shortest relaxation time, and its corresponding peak area, A1, remains the smallest, as confirmed by Chao et al. (2022). Bound water, characterized by its robust attachment to hydrophilic groups, demonstrates a fluidity that remains impervious to the effects of pre-treatment methodologies. Upon analysis of the T2 relaxation times, it was observed that the T22 values underwent a modest shift to the right following the application of pre-treatments. This discernible change suggests that the pre-treatment processes induced a partial loss of binding force in some of the immobilized water fractions. The shortened relaxation time of T23 was attributed to the high mobility of free water. This suggests that different pretreatment methods altered the water content and the ratio of free hydrogen protons in white radish (Chen et al., 2020).

During the pre-treatment phase, a reduction in the moisture content of the samples was observed. However, the relative proportions of the various moisture fractions exhibited distinct changes, with a notable increase in the proportion of weakly bound water (Fig. 1E). After pre-treatments, the relative area of A2 increased, the T2 range of the LC samples was lower than that of the TC samples, which may be due to the fact that the fiber orientation of the CL samples contributes to water migration, shorter relaxation time, and lower free water content and peak area. The greatest decrease in A3 in the ultrasound-assisted osmosis samples in this study was presumed due to the partial rupture of cell and vesicle membranes by ultrasound, which caused water migration from the vesicle membrane to the cytoplasm and promoted water migration from the inside to the outside, which promoted WL (Xu et al., 2021). And it was also suggested that the cavitation effect generated by ultrasound treatment accelerated the formation of microporous channels in the material and promoted the WL (Xu, Chen, et al., 2021). All pre-treatment samples of T23 move in a leftward order. The peak area A3 (free water area) decreases overall, with the largest decrease in ultrasound-assisted osmosis samples, which is consistent with the largest

WL obtained for the ultrasound-assisted osmosis samples. Blanching, osmosis, and ultrasound-assisted osmotic all reduced the free water content of the sample, but when the combined treatment of blanching and ultrasound-assisted osmosis, the reduction of A3 was not the greatest, which may be due to the blanching process of the sample to lose part of the water, the sample tissues caused a certain degree of damage to the destruction of the capillary tube, The entry of sugar solution after ultrasound-assisted osmotic treatment prevented some of the water loss.

3.2.2. DSC analysis

Tg' represents glass transition temperature (Aravindakshan, Nguyen, Kyomugasho, Van Loey, & Hendrickx, 2022). The Tg value of blanching samples group was the largest while blanching and ultrasound-assisted osmosis samples was the smallest (Fig. 1). The Tg' of blanching and ultrasound-assisted osmosis samples was reduced because the entry of small molecular sugars after osmotic pre-treatment, lowers the crystallization temperature of the system. The effect of blanching and osmotic treatment is opposite. Alterations in the water state within vegetable tissues were observed to have a close correlation with the glass transition temperature (Tg'). Furthermore, the available data strongly suggests that alterations in the state of water are accompanied by changes in the Tg'. However, the water state is linearly related to Tg' has not been reported. Based on the findings, the glass transition temperature (Tg') of vegetable tissues is influenced by both blanching and ultrasound-assisted osmosis. Future research could explore the linear relationship between the water state and Tg' in food systems, as well as the impact of combined processing techniques on the Tg' and overall quality of food products.

3.3. Multi-component analysis

The PCA score plot (Fig. 2A) for principal component analysis showed that scores in the same quadrant indicate a high degree of similarity (Joseph Bassey, Cheng, & Sun, 2022). And, from the confidence diagram (Fig. 2B) showed that there are large differences between fresh samples (there was no significant difference in the effect of pre-treatments methods on quality for transversal cutting piece/strip and longitudinal cutting piece/strip), with blanching samples, osmotic samples and ultrasound-assisted osmotic samples.

Cutting treatment on the positive axis of PC1 was highly positively correlated with the hardness, resilience, springiness, chewiness, gumminess and A3, which explains the maximum hardness and the highest free water content of fresh samples. The blanching and ultrasound-assisted osmosis treatment on the negative axis of PC1 was highly correlated with WL, SG, A2, and ΔE , which is consistent with the maximum SG obtained by blanching and ultrasound-assisted osmosis treatment in the previous section (Table 2). The blanching treatment on the negative axis of PC2 is negatively correlated with ΔE . The correlation analysis (Fig. 2D) showed a negative correlation between WL and hardness (-0.82), which further indicates an increase in WL and a decrease in hardness of the samples (Table 2), and a negative correlation between WL and A3 (-0.80), which is also consistent with the previously obtained maximum WL and minimum A3 for the ultrasound-assisted osmosis samples. Moreover, A3 was positively correlated with hardness (0.69), which explains the fresh sample had the highest free water content (A3) and the highest hardness. WL is positively correlated with SG, so the WL increasing of blanching and ultrasound-assisted osmosis samples. Furthermore, a significant positive correlation ($p < 0.05$) was observed between the variation of parameter A3 and the textural attributes (Fig. 1D). This finding suggests that the free water content serves as a critical determinant in assessing the quality characteristics of vegetable products.

Overall, we concluded that osmotic is the most effective method for color retention. The entry of osmotic substances into vegetables allows solutes from the osmotic solution to be absorbed into tissues (Bozkir

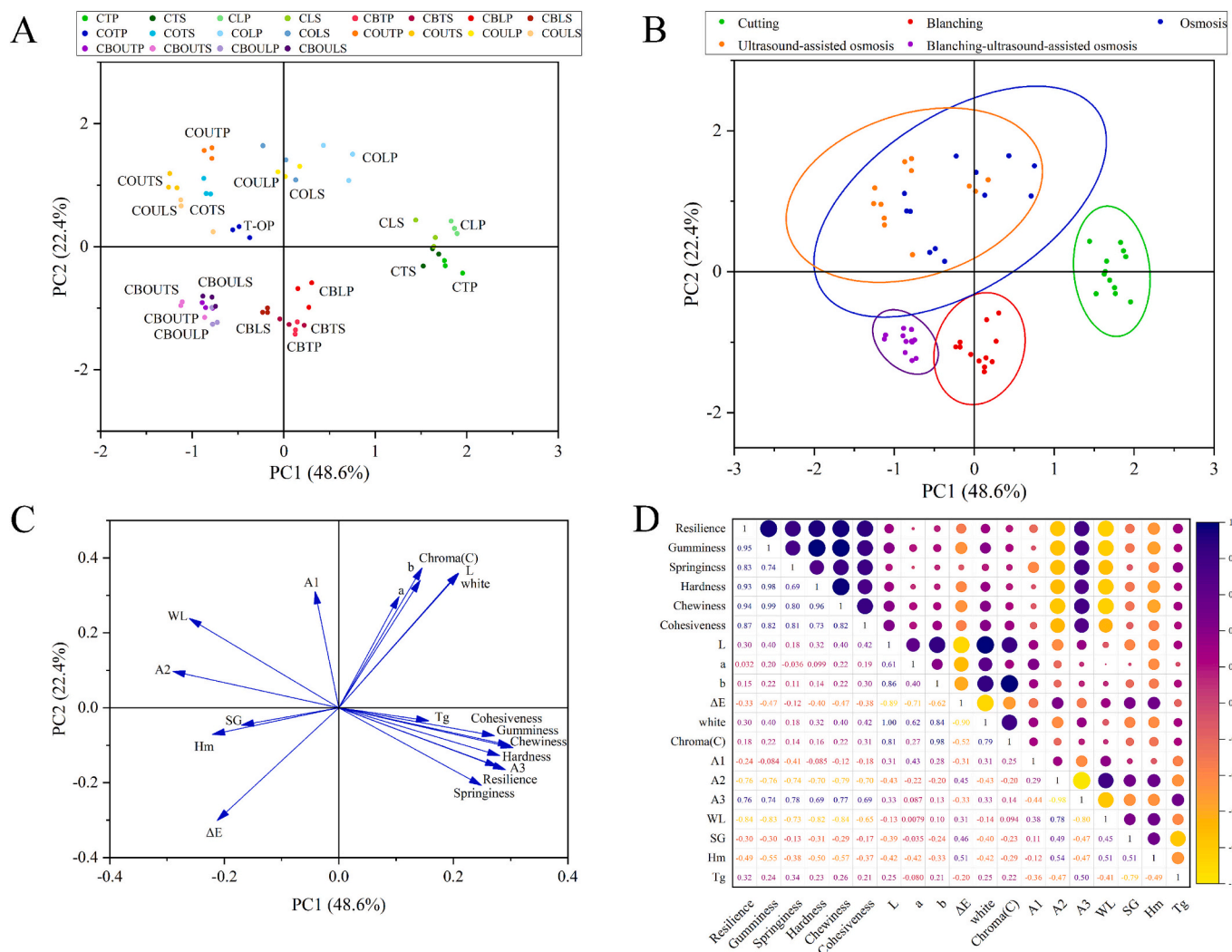


Fig. 2. PCA analysis and correlation analysis. (C: Cutting; T: Transversal; L: Longitudinal; P: Piece; S: Strip; B: Blanching; O: Osmotic; U: Ultrasound. The combination of capital letters represents joint processing. A: PCA score chart; B: PCA confidence map; C: PCA load chart; D: Correlation analysis chart).

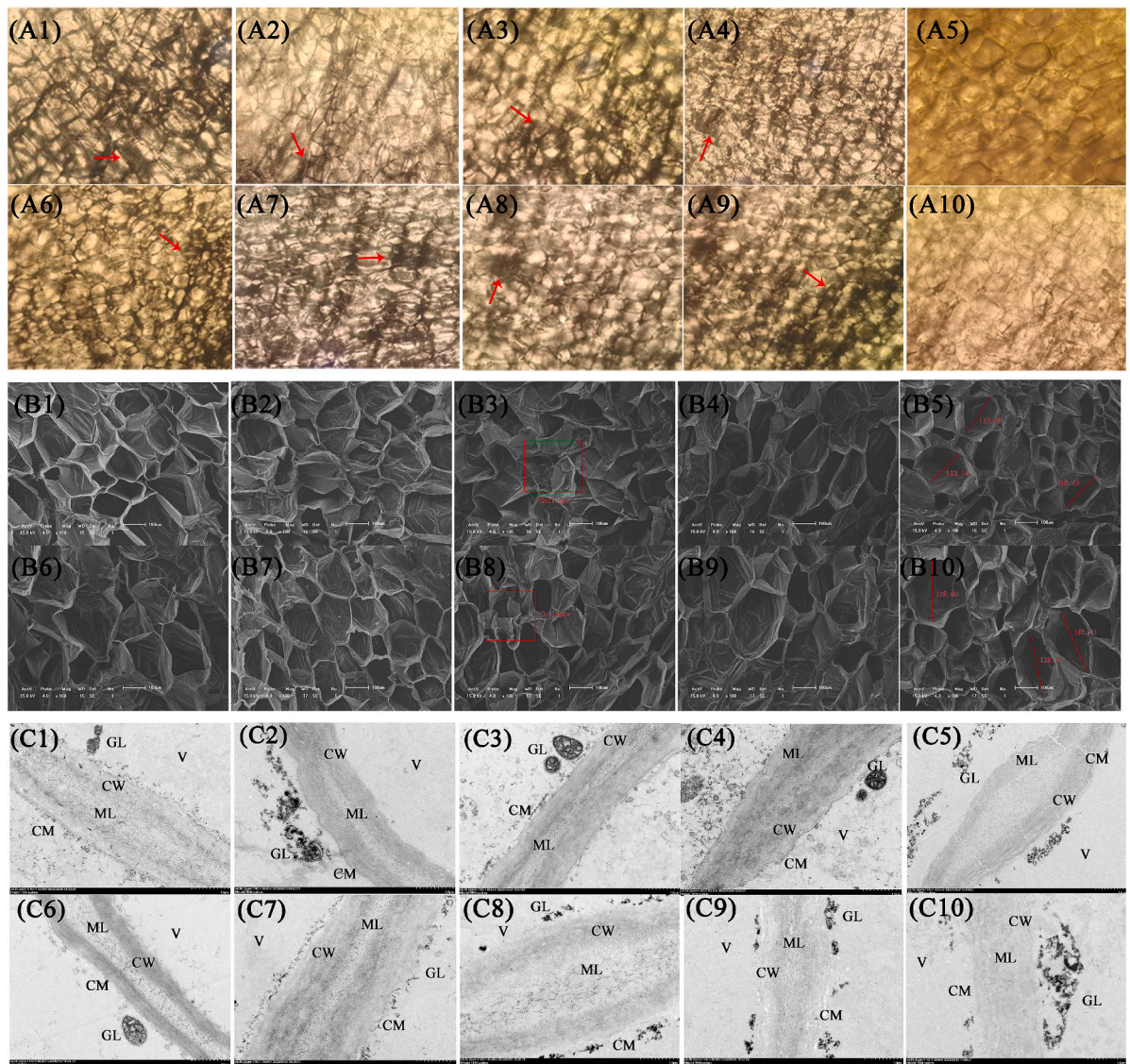
et al., 2019). It is worth considering pretreatment methods for vegetables that have a need to be dried and rehydrated (Sakooei-Vayghan, Peighambaroust, Hesari, & Peressini, 2020). The utilization of sophisticated osmotic solutions in conjunction with diverse processing methodologies for enhanced osmotic dehydration presents a valuable framework for the advancement of vegetable processing techniques. This approach may serve as a seminal reference for researchers and practitioners in the field (Miano, Rojas, & Augusto, 2021). We found an interesting phenomenon in this study. The increase of SG does not increase with the increase of WL, which may be related to the properties of the vegetables. Therefore, the increase in solids after penetration plays an important role in the next step of processing. In addition, the increase in SG maintains the volume of the dried sample (Kumar, Kalpana Devi, Panda, & Shrivastava, 2019). However, it should be noted that infiltration treatment may lead to a decrease in hardness. If there is a requirement for hardness in future vegetable production, changes in hardness ought to be considered as a top priority, rather than color. Blanching can be considered as a suitable pre-treatment method according to this study. Whether the requirements for other vegetables are consistent with this study needs to be further studied. The maximum ultrasonic penetration WL coincides with the maximum reduction in free water. Based on the current results, it can be inferred that the product requires drying during the processing stage (Obajemihi, Esua, Cheng, &

Sun, 2023). Therefore, ultrasonic-assisted osmotic pre-treatment may be considered for drying vegetables production.

3.4. Effect of pre-treatment on microstructural changes

3.4.1. Optical microscope analysis

Based on the results obtained earlier, TCP and TLP were selected for microstructural analysis. The extent of changes in cell characteristics of white radish after pre-treatment is shown in Fig. 3A1-A10 and Fig. 3D. Fresh TC and LC samples showed no significant differences, with uniform and intact cell size, visible cell gaps, and intracellular bubbles (red arrows). The untreated group of cutting samples had the largest amount of air, while after ultrasound treatment, the amount of air became smaller. This is consistent with the report of Liu, Wang, Lv, Li, and Wang (2021). After ultrasonic treatment, the cell wall is broken and ultrasonic microchannels are formed. Therefore, the intercellular air of all treated *platycodon grandiflorum* tissues is exhausted. The cell interstitial air was expelled and the cell shape was irregular after ultrasonic treatment. In contrast, in blanching and osmosis treatment, most of the samples had blurred cell boundaries, some cells lost water and became smaller, and the cell structure was altered. During blanching, vegetable tissues undergo profound cellular structural changes, which can enhance mass transfer and facilitate water transfer in the tissues (Deng et al., 2019),



D

| | Cutting | Blanching | Osmosis | Ultrasound-assisted osmosis | Blanching-ultrasound-assisted osmosis |
|--------------------------------|---------|-----------|---------|-----------------------------|---------------------------------------|
| Cell size uniformity | ***** | ***** | ***** | **** | ** |
| Cell boundary definition | ***** | **** | **** | ** | ** |
| Cell gap size | ** | *** | *** | ***** | ***** |
| Intracellular air volume | ***** | *** | *** | ** | * |
| Cell size uniformity | ***** | ***** | ***** | *** | ** |
| Cell boundary definition | ***** | *** | *** | *** | *** |
| Cell integrity | ***** | ** | ** | ** | ** |
| Pore uniformity | ***** | *** | *** | *** | ** |
| Cell membrane integrity | ***** | ** | *** | ** | * |
| Cell wall thickness | *** | *** | *** | *** | ** |
| Pectin layer thickness | ** | ** | ** | ***** | ***** |
| Glycogen particle distribution | * | ***** | ***** | *** | ***** |

Fig. 3. The pre-treatment of radish was observed by optical microscope, scanning electron microscope and transmission electron microscope. (C: Cutting; T: Transversal; L: Longitudinal; P: Piece; S: Strip; B: Blanching; O: Osmotic; U: Ultrasound. A1-A10: Optical microscopic observation of CTP, CBTP, COTP, COUTP, CBOU TP, CLP, CBTP, COTP, COUTP, CBOU TP. B1-B10: SEM of CTP, CBTP, COTP, COUTP, CBOU TP, CLP, CBTP, COTP, COUTP, CBOU TP respectively. C1-C10: TEM of CTP, CBTP, COTP, COUTP, CBOU TP, CLP, CBTP, COTP, COUTP, CBOU TP, respectively).

but the mechanism by which blanching accelerates mass transfer has not yet been thoroughly investigated.

In ultrasound-assisted osmosis treatment, the cell size varied. Furthermore, during blanching combined with ultrasound-assisted osmosis treatment, the cell gap widened, intracellular air was removed, microporous channels were formed, and deformation of cell shape occurred. In particular, the formation of microporous channels due to ultrasound increased the likelihood of cell structure destruction, resulting in a reduction in tissue hardness and cohesion, and consequently altering the textural properties of the samples (Wang et al., 2021). The pretreatment performed in this study altered the tissue structure of the samples, resulting in a decrease in their hardness after the pretreatment process (Table 2).

3.4.2. SEM analysis

The microstructural changes on the surface of the samples after different treatments observed by SEM (Fig. 3B1–B10 and Fig. 3D). Cell size uniformity was reduced after treatment compared to the untreated samples. The cell size difference was not significant between blanching and osmosis samples; the cell size uniformity of ultrasound-assisted osmosis samples and blanching and ultrasound-assisted osmosis samples cells was reduced and pores of different sizes were formed, which induced a greater probability of disintegration and affected the water migration changes. The pores of the blanching and ultrasound-assisted osmosis samples became larger, this may be due to the thermal disruption produced by blanching treatment and the microchannels generated by ultrasound making it easier for the osmotic solution to enter the sample tissue (Nowacka et al., 2019). The entry of the osmotic solution provides support to the skeleton of the cells, the osmotic solution has a protective effect on the sample tissue structure, the sample SG is the largest for ultrasound-assisted osmotic treatment. The formation of microchannels destroys the integrity of tissues and leads to the merger of adjacent cells, which leads to the enlargement of pore size (Carvalho, Perez-Palacios, & Ruiz-Carrascal, 2017).

Changes in the uniformity of cell size may be closely associated with cell rupture, which subsequently impacts water migration and alterations in water status (Xu, Chen, et al., 2021). The presence of large pores enhances water migration, which is in agreement with the previously observed greater water loss (WL) in samples that underwent both blanching and ultrasound-assisted osmosis, as well as those that only underwent ultrasound-assisted osmosis. In Xu's research (Xu et al., 2024), it was found that the cavitation and sponge effect of ultrasound caused cracks and collapses in the internal tissue of perilla leaves during the drying process, thereby facilitating water loss. This result is similar to the findings of our study. The cells in the blanching and ultrasound-assisted osmosis samples exhibit large pore sizes (Fig. 3D), and the extent of damage to the cell membrane from this pre-treatment increases with the size of the pores (Miano, Rojas, & Augusto, 2019).

3.4.3. TEM analysis

The microscopic changes of cell wall, cell membrane and organelles inside the cells of the samples after different treatments were observed by TEM (Fig. 3C1–C10 and Fig. 3D). The cutting samples exhibited smooth and uniformly thick cell walls, intact cell membranes, a consistent thickness of the middle cell layer (pectin layer), visible vesicle membranes, and intact intracellular glycogen granules (GL). The change of cell wall thickness after blanching treatment was not obvious, but the cell wall and cell membrane boundaries were blurred, GL were scattered, the vesicle (V) membrane disappeared, and the organelles were disintegrated, fragmented and free. Blanching pre-treatment affected the cell membranes, and the thermal effect increased the damage to the cell membranes (Wang et al., 2021). After the osmotic treatment, the organelles of CLP were more intact and glycogen granules (GL) were scattered in the CLP samples. The osmotic treatment had a protective effect on the tissue structure of the samples.

The middle layer (ML) of the cell locally becomes thicker of

ultrasound-assisted osmosis. The sponge effect in the ultrasonic treatment process permeates the tissue sample, inducing a sequence of rapid alternating compression and expansion, resulting in the creation of micropores and the distortion of the cell structure. The alterations induced in this process exert a significant influence on the ultimate physical and chemical attributes of the product. Moreover, the structural deformation encountered during this phase is a contributing factor to the water migration phenomenon (Deng et al., 2018), which is consistent with the large SG in ultrasound-assisted osmosis and blanching and ultrasound-assisted osmosis samples (Table 2). After pre-treatments, the changes of ML may be associated with alterations in both the content and molecular structure of the pectin component (Xu, Martinez, Yang, & Guo, 2020).

3.4.4. FT-IR analysis

The wider and stronger absorption peak at 3432 cm^{-1} is the telescopic vibration of the O–H bond (Fig. 4), which is caused by the intermolecular vibration of the galacturonic acid polymer backbone (Xu, Zhang, et al., 2021). The absorption peak at 1422 cm^{-1} indicates the stretching of the carboxylate anion ($-\text{COO}-$) group (Yan, Wu, Qiao, Cai, & Ma, 2019). The absorption peaks at $1300\text{--}1000\text{ cm}^{-1}$ are mainly generated by stretching vibration of C–O, representing C–OH and glycosidic bond C–O–C on the sugar ring. Absorption peaks at $1300\text{--}800\text{ cm}^{-1}$ are mainly indicate some change in the composition of monosaccharide (Xu et al., 2020). $900\text{--}888\text{ cm}^{-1}$ is a β -glycosidic bond (Li, Zhang, & Wang, 2020). The absorption peak at 770 cm^{-1} represents a phenyl group (Canteri, Renard, Le Bourvellec, & Bureau, 2019). The results of infrared qualitative analysis showed that the overall tensile vibration band strength of the total cell wall material after different pretreatments were similar and did not change significantly, but the changes in the internal composition of the cell wall such as glue and fiber were not clear. The future research should further delve into the changes of internal components within the cell wall, particularly focusing on key constituents such as colloids and fibers, to gain a more comprehensive understanding of the impact of pretreatment on the structure and function of the cell wall. By employing more sophisticated analytical techniques, such as two-dimensional infrared spectroscopy or isotope labeling, the specific mechanisms underlying the changes of these components during pretreatment can be elucidated.

The change of cell structure makes the components in the cell wall

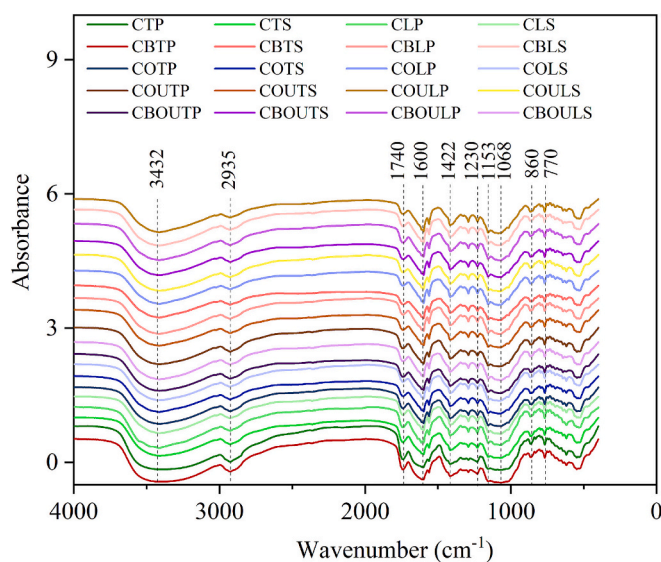


Fig. 4. FTIR spectrogram. (C: Cutting; T: Transversal; L: Longitudinal; P: Piece; S: Strip; B: Blanching; O: Osmotic; U: Ultrasound. The combination of capital letters represents joint processing).

change, such as pectin and hemicellulose in the cell wall degrade with the division of galacturonic acid chain structure, thus reducing the mechanical strength of the cell wall (An et al., 2023). The change of its mechanical properties (hardness and resistance) may change the retention and migration of water. Pre-treatment leads to irreversible loss of cell membrane integrity. Disruption of the cell wall structure reduces the resistance to water migration and speeds up drying time (An et al., 2023). In subsequent studies, the mechanism by which pre-treatment influences the structural alterations of vegetable tissues can be investigated through the lens of cell wall and cell membrane dynamics (Wang et al., 2023). By studying the internal components of cell wall after pre-treatment, such as functional groups such as gum and fiber, the content of pectin components, the molecular structure of pectin and the permeability and integrity of cell membrane to water migration, we can deeply explore product quality, water migration and microstructure of vegetables pre-treatment and provide methods for fine processing of vegetables. In addition, the processing technology and duration of pre-treatment should be strictly controlled according to the specific characteristics of vegetables (including the moisture distribution and migration direction of sample properties), so as to provide appropriate pretreatment methods according to the characteristics of the final product and obtain high-quality vegetable products.

4. Conclusion

Research on the pre-treatment of white radish has revealed that the cutting direction does not have a significant impact on its quality characteristics ($p > 0.05$). Samples that osmosis and ultrasound-assisted osmosis samples maintained the color well ($p < 0.05$). Ultrasound-assisted osmosis can be used as a pre-treatment for vegetables with high color requirements. Blanching has the least significant impact on the hardness of white radish ($p > 0.05$), while osmotic treatment has the greatest impact on hardness ($p < 0.05$). The samples subjected to blanching followed by ultrasound-assisted osmosis exhibited the largest increase in solid gain and water loss ($p < 0.05$), but their color was inferior to that of samples solely treated with ultrasound-assisted osmosis. The high degree of disruption to cell integrity can be considered as a method that facilitates the extraction of bioactive compounds. Blanching, osmotic treatment, and ultrasound-assisted osmosis all reduced the free water content of the samples. Correlation analysis revealed a negative correlation between water loss and hardness ($p < 0.05$) and a positive correlation between changes in free water and quality characteristics (hardness, viscosity, adhesiveness, and resilience) ($p < 0.05$). Infrared spectroscopy showed no significant change in the intensity of the total tensile vibration bands of the total cell wall after pretreatment. The microstructural changes in the pretreated samples affected the internal water distribution and product quality. This study focuses on white radish as the vegetable of research. In future studies, the processing techniques and time for pretreatment should be strictly controlled according to the specific characteristics of the vegetable (including the water distribution and migration direction of the sample properties), in order to provide suitable pretreatment methods based on the characteristics of the final product and obtain high-quality vegetable products. Moreover, further analysis can be conducted on the drying of pretreated products, including a comprehensive analysis of changes in nutritional components, microstructure, and other relevant aspects.

CRedit authorship contribution statement

Bixiang Wang: Writing – review & editing, Writing – original draft, Investigation, Formal analysis. **Yuanlong Jia:** Writing – review & editing, Formal analysis. **Yue Li:** Writing – review & editing, Investigation. **Xuan Jiao:** Writing – review & editing, Investigation. **Yang He:** Writing – review & editing, Project administration, Conceptualization. **Liankui Wen:** Writing – review & editing, Project administration, Conceptualization. **Zhitong Wang:** Writing – review & editing, Project

administration, Investigation.

Declaration of competing interest

The authors declare that they have no known competing financial interests or personal relationships that could have appeared to influence the work reported in this paper.

Acknowledgments

This work was supported by the Jilin Scientific and Technological Development Program (20230202047NC). And we also thank the Jilin Agricultural University Agricultural Products Processing and Storage Laboratory for support.

Data availability

Data will be made available on request.

References

- Ahmed, I., Qazi, I. M., & Jamal, S. (2016). Developments in osmotic dehydration technique for the preservation of fruits and vegetables. *Innovative Food Science & Emerging Technologies*, 34, 29–43. <https://doi.org/10.1016/j.foodchem.2020.128535>
- An, N. N., Lv, W. Q., Li, D., Wang, L. J., & Wang, Y. (2023). Effects of hot-air microwave rolling blanching pretreatment on the drying of turmeric (*Curcuma longa* L.): Physicochemical properties and microstructure evaluation. *Food Chemistry*, 398, Article 133925. <https://doi.org/10.1016/j.foodchem.2022.133925>
- An, N. N., Sun, W. H., Li, B. Z., et al. (2022). Effect of different drying techniques on drying kinetics, nutritional components, antioxidant capacity, physical properties and microstructure of edamame. *Food Chemistry*, 373, Article 131412. <https://doi.org/10.1016/j.foodchem.2021.131412>
- Andreou, V., Dimopoulos, G., Dermesonlouglou, E., & Taoukis, P. (2020). Application of pulsed electric fields to improve product yield and waste valorization in industrial tomato processing. *Journal of Food Engineering*, 270, Article 109778. <https://doi.org/10.1016/j.jfoodeng.2019.109778>
- Aravindakshan, S., Nguyen, T. H. A., Kyomugasho, C., van Loey, A., & Hendrickx, M. E. (2022). The rehydration attributes and quality characteristics of ‘quick-cooking’ dehydrated beans: Implications of glass transition on storage stability. *Food Research International*, 157, Article 111377. <https://doi.org/10.1016/j.foodres.2022.111377>
- Bozkir, H., Rayman Ergün, A., Serdar, E., Metin, G., & Baysal, T. (2019). Influence of ultrasound and osmotic dehydration pretreatments on drying and quality properties of persimmon fruit. *Ultrasonics Sonochemistry*, 54, 135–141. <https://doi.org/10.1016/j.ulsonch.2019.02.006>
- Canteri, M. H. G., Renard, C. M. G. C., le Bourvellec, C., & Bureau, S. (2019). ATR-FTIR spectroscopy to determine cell wall composition: Application on a large diversity of fruits and vegetables. *Carbohydrate Polymers*, 212, 186–196. <https://doi.org/10.1016/j.carbpol.2019.02.021>
- Carvalho, M. J., Perez-Palacios, T., & Ruiz-Carrascal, J. (2017). Physico-chemical and sensory characteristics of freeze-dried and air-dehydrated yogurt foam. *LWT*, 80, 328–334. <https://doi.org/10.1016/j.lwt.2017.02.039>
- Chao, E., Li, J., & Fan, L. (2022). Enhancing drying efficiency and quality of seed-used pumpkin using ultrasound, freeze-thawing and blanching pretreatments. *Food Chemistry*, 384, Article 132496. <https://doi.org/10.1016/j.foodchem.2022.132496>
- Chen, Y., Li, M., Dharmasiri, T. S. K., Song, X., Liu, F., & Wang, X. (2020). Novel ultrasonic-assisted vacuum drying technique for dehydrating garlic slices and predicting the quality properties by low field nuclear magnetic resonance. *Food Chemistry*, 306, Article 125625. <https://doi.org/10.1016/j.foodchem.2019.125625>
- Deng, L. Z., Mujumdar, A. S., Yang, X. H., Wang, J., Zhang, Q., Zheng, Z. A., ... Xiao, H. W. (2018). High humidity hot air impingement blanching (HHAIB) enhances drying rate and softens texture of apricot via cell wall pectin polysaccharides degradation and ultrastructure modification. *Food Chemistry*, 261, 292–300. <https://doi.org/10.1016/j.foodchem.2018.04.062>
- Deng, L. Z., Mujumdar, A. S., Zhang, Q., Yang, X. H., Wang, J., Zheng, Z. A., ... Xiao, H. W. (2019). Chemical and physical pretreatments of fruits and vegetables: Effects on drying characteristics and quality attributes—a comprehensive review. *Critical Reviews in Food Science and Nutrition*, 59(9), 1408–1432. <https://doi.org/10.1080/10408398.2017.1409192>
- Ding, T. H., Li, Y. C., Wang, J. L., Song, F. H., Jin, G. Y., Li, Z. F., ... Song, W. D. (2024). Effects of ultrasound blanching followed by hot air-coupled microwave drying on the quality of perilla leaves. *Journal of Stored Products Research*, 109, Article 102419. <https://doi.org/10.1016/j.jspr.2024.102419>
- Fan, K., & Zhang, M. (2019). Recent developments in the food quality detected by non-invasive nuclear magnetic resonance technology. *Critical Reviews in Food Science and Nutrition*, 59(14), 2202–2213. <https://doi.org/10.1080/10408398.2018.1441124>
- FAO, F. (2022). *Food and agriculture organization of the United Nations (FAO) report (last update: 2022.12.23)*. <https://www.fao.org/faostat/zh/#data/QCL>
- Jiang, J., Zhang, M., Devahastin, S., & Yu, D. (2021). Effect of ultrasound-assisted osmotic dehydration pretreatments on drying and quality characteristics of pulsed

- fluidized bed microwave freeze-dried strawberries. *LWT*, 145, Article 111300. <https://doi.org/10.1016/j.lwt.2021.111300>
- Joseph Bassey, E., Cheng, J. H., & Sun, D. W. (2022). Improving drying kinetics, physicochemical properties and bioactive compounds of red dragon fruit (*Hylocereus* species) by novel infrared drying. *Food Chemistry*, 375, Article 131886. <https://doi.org/10.1016/j.foodchem.2021.131886>
- Kumakura, K., Kato, R., Kobayashi, T., Sekiguchi, A., Kimura, N., Takahashi, H., Takahashi, A., & Matsuoka, H. (2017). Nutritional content and health benefits of sun-dried and salt-aged radish (takuan-zuke). *Food Chemistry*, 231, 33–41. <https://doi.org/10.1016/j.foodchem.2017.03.096>
- Kumar, V., Kalpana Devi, M., Panda, B., & Shrivastava, S. L. (2019). Shrinkage and rehydration characteristics of vacuum assisted microwave dried green bell pepper. *Journal of Food Process Engineering*, 42, Article e13030. <https://doi.org/10.1111/jfpe.13030>
- Li, J. T., Wei, Y. W., Wang, M. Y., Yan, C. X., Ren, X., & Fu, X. J. (2021). Antibacterial activity prediction model of traditional chinese medicine based on combined data-driven approach and machine learning algorithm: Constructed and validated. *Frontiers in Microbiology*, 12, Article 763498. <https://doi.org/10.3389/fmicb.2021.763498>
- Li, L., Zhang, M., & Wang, W. (2020). Ultrasound-assisted osmotic dehydration pretreatment before pulsed fluidized bed microwave freeze-drying (PFBMFD) of Chinese yam. *Food Bioscience*, 35, Article 100548. <https://doi.org/10.1016/j.fbio.2020.100548>
- Liu, Y. Y., Wang, Y., Lv, W. Q., Li, D., & Wang, L. J. (2021). Freeze-thaw and ultrasound pretreatment before microwave combined drying affects drying kinetics, cell structure and quality parameters of *Platycodon grandiflorum*. *Industrial Crops and Products*, 164, Article 113391. <https://doi.org/10.1016/j.indcrop.2021.113391>
- Luo, S., An, R., Zhou, H., Zhang, Y., Ling, J., Hu, H., & Li, P. (2022). The glucosinolate profiles of brassicaceae vegetables responded differently to quick-freezing and drying methods. *Food Chemistry*, 383, Article 132624. <https://doi.org/10.1016/j.foodchem.2022.132624>
- Miano, A. C., Rojas, M. L., & Augusto, P. E. D. (2019). Structural changes caused by ultrasound pretreatment: Direct and indirect demonstration in potato cylinders. *Ultrasonics Sonochemistry*, 52, 176–183. <https://doi.org/10.1016/j.ultsonch.2018.11.015>
- Miano, A. C., Rojas, M. L., & Augusto, P. E. D. (2021). Combining ultrasound, vacuum and/or ethanol as pretreatments to the convective drying of celery slices. *Ultrasonics Sonochemistry*, 79, Article 105779. <https://doi.org/10.1016/j.ultsonch.2021.105779>
- Nokuthula, A. N., Sephora, M. M., Faith, S., & Dharini, S. (2024). Impact of different pretreatments and drying methods on the physicochemical properties, bioactive compounds and antioxidant activity of different tomato (*Solanum lycopersicum*) cultivars. *LWT*, 207, Article 116641. <https://doi.org/10.1016/j.lwt.2024.116641>
- Nowacka, M., Laghi, L., Rybak, K., Dalla Rosa, M., Witrowa-Rajchert, D., & Tylewicz, U. (2019). Water state and sugars in cranberry fruits subjected to combined treatments: Cutting, blanching and sonication. *Food Chemistry*, 299, Article 125122. <https://doi.org/10.1016/j.foodchem.2019.125122>
- Obajemihi, O. I., Esua, O. J., Cheng, J. H., & Sun, D. W. (2023). Effects of pretreatments using plasma functionalized water, osmodehydration and their combination on hot air drying efficiency and quality of tomato (*Solanum lycopersicum* L.) slices. *Food Chemistry*, 406, Article 134995. <https://doi.org/10.1016/j.foodchem.2022.134995>
- Ozen, B. F., Dock, L. L., Ozdemir, M., & Floros, J. D. (2002). Processing factors affecting the osmotic dehydration of diced green peppers. *International Journal of Food Science & Technology*, 37, 497–502. <https://doi.org/10.1046/j.1365-2621.2002.00606.x>
- Rojas, M. L., Silveira, I., & Augusto, P. E. D. (2019). Improving the infrared drying and rehydration of potato slices using simple approaches: Perforations and ethanol. *Journal of Food Process Engineering*, 42, Article e13089. <https://doi.org/10.1111/jfpe.13089>
- Sakooei-Vayghan, R., Peighambaridoust, S. H., Hesari, J., & Peressini, D. (2020). Effects of osmotic dehydration (with and without sonication) and pectin-based coating pretreatments on functional properties and color of hot-air dried apricot cubes. *Food Chemistry*, 311, Article 125978. <https://doi.org/10.1016/j.foodchem.2019.125978>
- Shafiq, F. A., Krishna, H. C., Mushrif, S. K., Ramegowda, G. K., Bhuvaneshwari, S., Shankarappa, T. H., & Ahmad, S. N. (2022). Effects of pre-treatments and drying methods on drying kinetics and physical properties of raisins. *Biological Forum—An International Journal*, 14, 155–160.
- Tao, Y., Han, M., Gao, X., et al. (2019). Applications of water blanching, surface contacting ultrasound-assisted air drying, and their combination for dehydration of white cabbage: Drying mechanism, bioactive profile, color and rehydration property. *Ultrasonics Sonochemistry*, 53, 192–201. <https://doi.org/10.1016/j.ultsonch.2019.01.003>
- Wang, B. X., Jia, Y. L., Li, Y., Wang, Z. T., Wen, L. K., He, Y., & Xu, X. Y. (2023). Dehydration–rehydration vegetables: Evaluation and future challenges. *Food Chemistry: X*, 20, Article 100935. <https://doi.org/10.1016/j.fochx.2023.100935>
- Wang, B. X., Li, Y., Lv, Y. C., Jiao, X., Wang, Z. T., He, Y., & Wen, L. K. (2023). Dehydration–rehydration mechanism of vegetables at the cell-wall and cell-membrane levels and future research challenges. *Critical Reviews in Food Science and Nutrition*. <https://doi.org/10.1080/10408398.2023.2233620>
- Wang, H., Fang, X. M., Sutar, P. P., Meng, J. S., Wang, J., Yu, X. L., & Xiao, H. W. (2021). Effects of vacuum-steam pulsed blanching on drying kinetics, colour, phytochemical contents, antioxidant capacity of carrot and the mechanism of carrot quality changes revealed by texture, microstructure and ultrastructure. *Food Chemistry*, 338, Article 127799. <https://doi.org/10.1016/j.foodchem.2020.127799>
- Wang, J., Chen, Y. X., Wang, H., Wang, S. Y., Lin, Z., Zhao, L. L., & Xu, H. D. (2022). Ethanol and blanching pretreatments change the moisture transfer and physicochemical properties of apple slices via microstructure and cell-wall polysaccharides nanostructure modification. *Food Chemistry*, 381, Article 132274. <https://doi.org/10.1016/j.foodchem.2022.132274>
- Wang, J., Fang, X. M., Mujumdar, A. S., et al. (2017). Effect of high-humidity hot air impingement blanching (HHAIB) on drying and quality of red pepper (*Capsicum annum* L.). *Food Chemistry*, 220, 145–152. <https://doi.org/10.1016/j.foodchem.2016.09.200>
- Xu, B., Chen, J., Sylvain Tiliwa, E., Yan, W., Roknul Azam, S. M., Yuan, J., ... Ma, H. (2021). Effect of multi-mode dual-frequency ultrasound pretreatment on the vacuum freeze-drying process and quality attributes of the strawberry slices. *Ultrasonics Sonochemistry*, 78, Article 105714. <https://doi.org/10.1016/j.ultsonch.2021.105714>
- Xu, F., Jin, X., Zhang, L., & Chen, X. D. (2017). Investigation on water status and distribution in broccoli and the effects of drying on water status using NMR and MRI methods. *Food Research International*, 96, 191–197. <https://doi.org/10.1016/j.foodres.2017.03.041>
- Xu, K., Martinez, M. M., Yang, B., & Guo, M. (2020). Fine structure, physicochemical and antioxidant properties of LM-pectins from okra pods dried under different techniques. *Carbohydrate Polymers*, 241, Article 116272. <https://doi.org/10.1016/j.carbpol.2020.116272>
- Xu, X., Zhang, L., Yagoub, A. E. A., Yu, X., Ma, H., & Zhou, C. (2021). Effects of ultrasound, freeze-thaw pretreatments and drying methods on structure and functional properties of pectin during the processing of okra. *Food Hydrocolloids*, 120, Article 106965. <https://doi.org/10.1016/j.foodhyd.2021.106965>
- Xu, Y. R., Wan, F. X., Zang, Z. P., Jiang, C. H., Wang, T. X., Shang, J. W., & Huang, X. P. (2024). Effect of different pretreatment methods on drying characteristics and quality of wolfberry (*Lycium barbarum*) by radio frequency-hot air combined segmented drying. *Food and Bioprocess Technology*, 1–15. <https://doi.org/10.1007/s11947-024-03340-0>
- Yan, J. K., Wu, L. X., Qiao, Z. R., Cai, W. D., & Ma, H. (2019). Effect of different drying methods on the product quality and bioactive polysaccharides of bitter melon (*Momordica charantia* L.) slices. *Food Chemistry*, 271, 588–596. <https://doi.org/10.1016/j.foodchem.2018.08.012>
- Zhang, L., Liao, L., Qiao, Y., Wang, C., Shi, D., An, K., & Hu, J. (2020). Effects of ultrahigh pressure and ultrasound pretreatments on properties of strawberry chips prepared by vacuum-freeze drying. *Food Chemistry*, 303, Article 125386. <https://doi.org/10.1016/j.foodchem.2019.125386>
- Zhou, Y. H., Vidyarthi, S. K., Zhong, C. S., Zheng, Z. A., An, Y., Wang, J., ... Xiao, H. W. (2020). Cold plasma enhances drying and color, rehydration ratio and polyphenols of wolfberry via microstructure and ultrastructure alteration. *LWT*, 134, Article 110173. <https://doi.org/10.1016/j.lwt.2020.110173>